Available online at www.sciencedirect.com
SCIENCE DIRECT
Engineering Structures 28 (2006) 43–53
ENGINEERING STRUCTURES
www.elsevier.com/locate/engstruct

Optimal design theories and applications of tuned mass dampers

Chien-Liang Lee[a,*], Yung-Tsang Chen[b], Lap-Loi Chung[c], Yen-Po Wang[d]

[a] *Natural Hazard Mitigation Research Center, National Chiao-Tung University, 1001 Ta Hsueh Road, Hsinchu 300, Taiwan, ROC*
[b] *Department of Civil and Environmental Engineering, University of California, Davis, 1 Shields Avenue, CA 95616, USA*
[c] *National Center for Research on Earthquake Engineering, 200, Section 3, HsinHai Road, Taipei 106, Taiwan, ROC*
[d] *Department of Civil Engineering, National Chiao-Tung University, 1001 Ta Hsueh Road, Hsinchu 300, Taiwan, ROC*

Received 20 August 2004; received in revised form 14 June 2005; accepted 21 June 2005
Available online 19 August 2005

Abstract

An optimal design theory for structures implemented with tuned mass dampers (TMDs) is proposed in this paper. Full states of the dynamic system of multiple-degree-of-freedom (MDOF) structures, multiple TMDs (MTMDs) installed at different stories of the building, and the power spectral density (PSD) function of environmental disturbances are taken into account. This proposed method allows for a more extensive application and successfully releases the limitations based on simplified models. The optimal design parameters of TMDs in terms of the damping coefficients and spring constants corresponding to each TMD are determined through minimizing a performance index of structural responses defined in the frequency domain. Moreover, a numerical method is also proposed for searching for the optimal design parameters of MTMDs in a systematic fashion such that the numerical solutions converge monotonically and effectively toward the exact solutions as the number of iterations increases. The feasibility of the proposed optimal design theory is verified by using a SDOF structure with a single TMD (STMD), a five-DOF structure with two TMDs, and a ten-DOF structure with a STMD.

Keywords: Multiple tuned mass damper; Optimal design; Passive control

1. Introduction

A tuned mass damper, consisting of a mass, damping, and a spring, is an effective and reliable structural vibration control device commonly attached to a vibrating primary system for suppressing undesirable vibrations induced by winds and earthquake loads. The natural frequency of the TMD is tuned in resonance with the fundamental mode of the primary structure, so that a large amount of the structural vibrating energy is transferred to the TMD and then dissipated by the damping as the primary structure is subjected to external disturbances. Consequently, the safety and habitability of the structure are greatly enhanced. The TMD system has been successfully installed in slender skyscrapers and towers to suppress the wind-induced structural dynamic responses [1,2]; such structures include the CN Tower (535 m) in Canada, the John Hancock Building (sixty stories) in Boston, Center-Point Tower (305 m) in Sydney, and the tallest building in the world, Taipei 101 Tower (101 stories, 504 m) [3] in Taiwan. From the field vibration measurements, it has been proved that a TMD is an effective and feasible system to use in structural vibration control against high wind loads.

Frahm [4] proposed the TMD system in 1909 for reducing the mechanical vibration induced by monotonic harmonic forces. It is found that if a secondary system composed of a mass, a damping device, and a spring is implemented on a primary structure and its natural frequency is tuned to be very close to the dominant mode of the primary structure, a large reduction in the dynamic responses of the primary structure can be achieved. Although the basic design concept of the TMD is quite simple, the parameters (mass, damping, and stiffness) of the TMD system must be obtained through optimal design procedures to attain a better control performance. Therefore, the determination of optimal design

* Corresponding author. Tel.: +886 3 5731936; fax: +886 3 5713221.
E-mail address: link.cv92g@nctu.edu.tw (C.-L. Lee).

0141-0296/$ - see front matter © 2005 Elsevier Ltd. All rights reserved.
doi:10.1016/j.engstruct.2005.06.023

Nomenclature

$\mathbf{a}_i$	location vector of the mass for the i-th TMD
$\mathbf{b}_i$	location vector of the damping and stiffness for the i-th TMD
$\mathbf{C}$	damping matrix of the passive controlled structure
$\mathbf{C}_s$	damping matrix of the structure
c_{di}	damping of the i-th TMD
c_s	damping of the SDOF structure
$\mathbf{D}$	location matrix of the partial responses
d	difference of the upper bound and lower bound of the incremental step
$\mathbf{E}$	the location matrix of the external disturbances (with a TMD)
$\mathbf{E}_s$	location matrix of the external disturbances
$\mathbf{e}$	the location matrix of the external disturbances for the SDOF structure
f	frequency (Hz)
f_{opt}	optimal frequency ratio of the TMD (TMD's frequency/structure's frequency)
$\mathbf{H}(\omega)$	frequency response function (transfer function)
$\mathbf{I}$	identity matrix
J	performance index
j	$\sqrt{-1}$
$\mathbf{K}$	stiffness matrix of the passive controlled structure
$\mathbf{K}_s$	stiffness matrix of the structure
k_{di}	stiffness of the i-th TMD
k_s	stiffness of the SDOF structure
$\mathbf{M}$	mass matrix of the passive controlled structure
$\mathbf{M}_s$	mass matrix of the structure
m_{di}	mass of the i-th TMD
n	degrees of freedom of the structure
p	total number of TMDs
$p_{kk}(\omega)$	the k-th diagonal elements of the square matrices $\mathbf{P}(\omega)$
q	total number of external disturbances
$q_{kk}(\omega)$	the k-th diagonal elements of the square matrices $\mathbf{Q}(\omega)$
$\mathbf{S}_{\text{WW}}(\omega)$	PSD function matrix of the external disturbance vector $\mathbf{w}(t)$
$\mathbf{S}_{\text{YY}}(\omega)$	PSD function matrix of the partial response vector $\mathbf{y}(t)$
$S_u(\omega)$	Davenport along-wind speed spectrum
s_{ci}	step of the increments for the parameters c_{di}
s_{ki}	step of the increments for the parameters k_{di}
s_l	lower bound of the incremental step
s_u	upper bound of the incremental step
S_0	constant PSD function of a white noise signal
T	transpose of a matrix or vector (or transpose and complex conjugate of a matrix or vector)
$\mathbf{w}(t)$	external disturbance vector
$\mathbf{W}(\omega)$	Fourier transform of the external disturbance vector
$\mathbf{X}(\omega)$	Fourier transform of the displacement vector of the passive controlled system
$\mathbf{x}(t)$	displacement vector of the passive controlled structure
$\mathbf{x}_s(t)$	displacement vector of the structure
$x_d(t)$	stroke of the TMD
$\mathbf{y}(t)$	the partial response vector of the structure
δ	prescribed tolerance
ξ_{opt}	optimal damping ratio of the TMD
μ	mass ratio (TMD's mass/main structure's total mass)
ω	circular frequency of the passive controlled system
ρ	golden ratio

parameters of the TMD to enhance the control effectiveness has become very crucial.

Since Den Hartog [5] first proposed an optimal design theory for the TMD for an undamped single-degree-of-freedom (SDOF) structure, many optimal design methods for the TMD have been developed to control the structural vibration induced by various types of excitation source [6–10]. Crandall and Mark [7] adopted the random vibration theory to analyze a SDOF structure implemented with a single TMD (STMD) subjected to white noise base excitation. The results demonstrated that the TMD could effectively reduce the vibration of the base-excited structure. Warburton et al. [8,9] further proposed optimal design formulas for the TMD system under different types of load, such as harmonic forces, wind loads, and seismic loads. However, the control effectiveness is highly sensitive to the design parameters of the TMD relative to the parameters of the primary structure. If the design parameters of the TMD deviate from the optimal design values or error exists in the identification of the natural frequency of the primary structure, a detuning effect will occur and the control effectiveness may deteriorate. Hence, the adoption of multiple tuned mass dampers (MTMDs) [10–23] with distributed natural frequencies around the controlled modes (horizontal or torsional motions) of the primary structure has been proposed to alleviate the detuning effect or to enhance the control performance.

In the above-mentioned studies, the design parameters of MTMDs are determined through parametric studies or by their proposed optimal design methods. Moreover, the external disturbances considered in these studies are limited to white noise and harmonic force over a frequency range, or random signals, such as earthquake excitations as studied by Li et al. [15–19]. In addition, Stech [22] adopted a H_2-based approach for optimally tuning the passive vibration absorbers to control both the torsional mode and the bending

mode of a mass reactive T (MRT) structure. Zuo et al. [23] proposed a minimax optimal design method for vibration control of a free–free beam implemented with a 3-DOF TMD or with three SDOF TMDs.

In this paper, an optimal design theory with a systematic and efficient procedure for searching for the optimal design parameters for the TMD is proposed. Full states of the dynamic system of MDOF structures, multiple TMDs installed at different stories of the building, and the PSD function of environmental disturbances are taken into account. Since the sufficient and necessary conditions are highly nonlinear simultaneous equations, a numerical method for the optimal design theory of the TMD is proposed in this paper such that the solution of the optimal design parameters converges monotonically toward the exact solutions as the number of iterations increases. Finally, the feasibility of the proposed optimal design theory and the numerical scheme is verified through the numerical simulations of a full-order five-DOF structure and a ten-DOF structure installed with two TMDs and a STMD, respectively.

2. Derivation of optimal design theory

When a structure with n degrees of freedom (DOF) is subjected to external disturbances, $\mathbf{w}(t)$, its equation of motion can be described as

$$\mathbf{M}_s\ddot{\mathbf{x}}_s(t) + \mathbf{C}_s\dot{\mathbf{x}}_s(t) + \mathbf{K}_s\mathbf{x}_s(t) = \mathbf{E}_s\mathbf{w}(t) \tag{1}$$

where $\mathbf{x}_s(t)$ is the $n\times 1$ displacement vector, $\mathbf{w}(t)$ is the $q\times 1$ external disturbance vector, q is the number of disturbances, $\mathbf{M}_s$, $\mathbf{C}_s$ and, $\mathbf{K}_s$ are the $n\times n$ mass, damping, and stiffness matrices, respectively, and $\mathbf{E}_s$ is the $n\times q$ location matrix of external disturbances. If MTMDs are implemented in this MDOF structure to suppress the structural vibration induced by the external disturbances, the governing equation of the passive controlled system can be taken as

$$\mathbf{M}\ddot{\mathbf{x}}(t) + \mathbf{C}\dot{\mathbf{x}}(t) + \mathbf{K}\mathbf{x}(t) = \mathbf{E}\mathbf{w}(t) \tag{2}$$

where $\mathbf{x}(t) = \begin{bmatrix}\mathbf{x}_s(t)\\ \mathbf{x}_d(t)\end{bmatrix}$ is the $(n+p)\times 1$ displacement vector of the passive controlled system, $\mathbf{M} = \begin{bmatrix}\mathbf{M}_s & \mathbf{0}\\ \mathbf{0} & \mathbf{0}\end{bmatrix} + \sum_{i=1}^{p} m_{di}\mathbf{a}_i\mathbf{a}_i^{\mathrm{T}}$, $\mathbf{C} = \begin{bmatrix}\mathbf{C}_s & \mathbf{0}\\ \mathbf{0} & \mathbf{0}\end{bmatrix} + \sum_{i=1}^{p} c_{di}\mathbf{b}_i\mathbf{b}_i^{\mathrm{T}}$ and $\mathbf{K} = \begin{bmatrix}\mathbf{K}_s & \mathbf{0}\\ \mathbf{0} & \mathbf{0}\end{bmatrix} + \sum_{i=1}^{p} k_{di}\mathbf{b}_i\mathbf{b}_i^{\mathrm{T}}$ are, respectively, the $(n+p)\times(n+p)$ mass, damping and stiffness matrices of the passive controlled system, p is the total number of TMDs installed in the structure, m_{di}, c_{di}, k_{di} are the mass, damping and stiffness of the i-th TMD, respectively, $\mathbf{a}_i$ is the $(n+p)\times 1$ location vector of the mass for the i-th TMD, $\mathbf{b}_i$ is the $(n+p)\times 1$ location vector of the damping and stiffness for the i-th TMD, $\mathbf{E}$ is the $(n+p)\times q$ location matrix of the external disturbances and the superscript T denotes the transpose of a matrix or vector.

To derive the optimal design parameters of the TMD more generally, this study may consider the partial responses of the structure instead of using the full ones as

$$\mathbf{y}(t) = \mathbf{D}\mathbf{x}(t) \tag{3}$$

where $\mathbf{y}(t)$ is the $r\times 1$ partial response vector of the structure and $\mathbf{D}$ is the $r\times(n+p)$ location matrix of these partial responses. If the location matrix $\mathbf{D} = \begin{bmatrix}\mathbf{I}_n & \mathbf{0}\end{bmatrix}$ is adopted, the partial response vector $\mathbf{y}(t)$ becomes the full displacement vector of the structure $\mathbf{x}_s(t)$.

Taking a Fourier transform to both sides of the passive control Eq. (2), the relation of the system response vector $\mathbf{x}(t)$ and the external disturbance vector $\mathbf{w}(t)$ in the frequency domain takes the form

$$\begin{aligned}\mathbf{X}(\omega) &= [-\omega^2\mathbf{M} + j\omega\mathbf{C} + \mathbf{K}]^{-1}\mathbf{E}\mathbf{W}(\omega)\\ &= \mathbf{H}(\omega)\mathbf{E}\mathbf{W}(\omega)\end{aligned} \tag{4}$$

where $\mathbf{H}(\omega) = [-\omega^2\mathbf{M} + j\omega\mathbf{C} + \mathbf{K}]^{-1}$ is the $(n+p)\times(n+p)$ frequency response function and $j = \sqrt{-1}$. Similarly, the relation between the partial response vector of the structure $\mathbf{y}(t)$ and the external disturbance vector $\mathbf{w}(t)$ in the frequency domain can be expressed as

$$\mathbf{Y}(\omega) = \mathbf{D}\mathbf{X}(\omega) = \mathbf{D}\mathbf{H}(\omega)\mathbf{E}\mathbf{W}(\omega). \tag{5}$$

If the external disturbance vector, $\mathbf{w}(t)$, is a random signal, the partial response of the structure $\mathbf{y}(t)$ is also a random one, and their PSD functions can be written as

$$\mathbf{S}_{\mathrm{YY}}(\omega) = \mathbf{D}\mathbf{H}(\omega)\mathbf{E}\mathbf{S}_{\mathrm{WW}}(\omega)\mathbf{E}^{\mathrm{T}}\mathbf{H}^{\mathrm{T}}(\omega)\mathbf{D}^{\mathrm{T}} \tag{6}$$

where $\mathbf{S}_{\mathrm{YY}}(\omega)$ is the $r\times r$ PSD function matrix of the partial response vector $\mathbf{y}(t)$, $\mathbf{S}_{\mathrm{WW}}(\omega)$ is the $q\times q$ PSD function matrix of the external disturbance vector $\mathbf{w}(t)$ and the superscript T denotes the transpose or the complex conjugate of a matrix or vector. Since the integral of the PSD function of the structural response with respect to frequency is the mean square value of the structural response, the performance index for the optimization of the TMD design parameters in this study is therefore defined as

$$\begin{aligned}J &= \int_{-\infty}^{\infty}\mathrm{tr}\{\mathbf{S}_{\mathbf{YY}}(\omega)\}\mathrm{d}\omega\\ &= \int_{-\infty}^{\infty}\mathrm{tr}\{\mathbf{D}\mathbf{H}(\omega)\mathbf{E}\mathbf{S}_{\mathrm{WW}}(\omega)\mathbf{E}^{\mathrm{T}}\mathbf{H}^{\mathrm{T}}(\omega)\mathbf{D}^{\mathrm{T}}\}\mathrm{d}\omega\end{aligned} \tag{7}$$

where $\mathrm{tr}\{\bullet\}$ is the trace of a square matrix.

Because the frequency response function $\mathbf{H}(\omega)$ expressed in Eq. (4) is a function of the damping (c_{di}) and the stiffness (k_{di}) of the TMD, the partial differentials of the frequency response function with respect to each design parameter are represented, respectively, as

$$\frac{\partial\mathbf{H}(\omega)}{\partial c_{di}} = -j\omega\mathbf{H}(\omega)\mathbf{b}_i\mathbf{b}_i^{\mathrm{T}}\mathbf{H}(\omega), \quad i = 1, 2, \ldots, p \tag{8a}$$

$$\frac{\partial\mathbf{H}(\omega)}{\partial k_{di}} = -\mathbf{H}(\omega)\mathbf{b}_i\mathbf{b}_i^{\mathrm{T}}\mathbf{H}(\omega), \quad i = 1, 2, \ldots, p \tag{8b}$$

Since the PSD function matrix $\mathbf{S}_{\mathrm{YY}}(\omega)$ of the structural responses is a positive-definite matrix, the sufficient and

necessary conditions are

$$\frac{\partial J}{\partial c_{di}} = -\int_{-\infty}^{\infty} \mathrm{tr}\{\mathbf{P}(\omega) + \mathbf{P}^{\mathrm{T}}(\omega)\}\mathrm{d}\omega = -\int_{-\infty}^{\infty} \sum_{k=1}^{r} \{p_{kk}(\omega) + p_{kk}^{*}(\omega)\}\mathrm{d}\omega = 0, \quad i = 1, 2, \ldots, p \tag{9a}$$

$$\frac{\partial J}{\partial} k_{di} = -\int_{-\infty}^{\infty} \mathrm{tr}\{\mathbf{Q}(\omega) + \mathbf{Q}^{\mathrm{T}}(\omega)\}\mathrm{d}\omega = -\int_{-\infty}^{\infty} \sum_{k=1}^{r} \{q_{kk}(\omega) + q_{kk}^{*}(\omega)\}\mathrm{d}\omega = 0, \quad i = 1, 2, \ldots, p \tag{9b}$$

where

$$\mathbf{P}(\omega) = j\omega \mathbf{D}\mathbf{H}(\omega)\mathbf{b}_i\mathbf{b}_i^{\mathrm{T}}\mathbf{H}(\omega)\mathbf{E}\mathbf{S}_{\mathbf{WW}}(\omega)\mathbf{E}^{\mathrm{T}}\mathbf{H}^{\mathrm{T}}(\omega)\mathbf{D}^{\mathrm{T}} \tag{10a}$$

$$\mathbf{Q}(\omega) = \mathbf{D}\mathbf{H}(\omega)\mathbf{b}_i\mathbf{b}_i^{\mathrm{T}}\mathbf{H}(\omega)\mathbf{E}\mathbf{S}_{\mathbf{WW}}(\omega)\mathbf{E}^{\mathrm{T}}\mathbf{H}^{\mathrm{T}}(\omega)\mathbf{D}^{\mathrm{T}} \tag{10b}$$

in which, $\mathbf{H}^{\mathrm{T}}(\omega)$ denotes $[\mathbf{H}^{*}(\omega)]^{\mathrm{T}}$, $p_{kk}(\omega)$ and $q_{kk}(\omega)$ are, respectively, the k-th diagonal elements of the $r \times r$ square matrices, $\mathbf{P}(\omega)$ and $\mathbf{Q}(\omega)$, and the superscript * denotes the complex conjugate of a complex number. The $2p$ unknown optimal design parameters of the TMD (c_{di} and k_{di}) can be solved from the $2p$ simultaneous equations (Eqs. (9a) and (9b)) by the proposed numerical method as will be discussed later.

3. Numerical methods for optimal design theory

The sufficient and necessary condition for the optimization of the TMD parameters is a set of highly nonlinear simultaneous equations (Eqs. (9a) and (9b)). As a result, the exact solutions of the optimal design parameters are difficult to obtain, except for the simple systems, such as the undamped SDOF structure implemented with a STMD. This paper proposes a numerical method for determining the optimal design parameters for the TMD in a systematic fashion by which the results converge monotonically toward the exact solutions with each iteration. Firstly, a set of initial values, $c_{di}^{(1)}$ and $k_{di}^{(1)}$, $i = 1, 2, \ldots, p$, is guessed and in turn substituted into Eq. (7) to obtain the initial value $J^{(1)}$ of the performance index. Let $\mathrm{d}J^{(1)}$ be the difference between the updated value $J^{(2)}$ and the initial value $J^{(1)}$ of the performance index; their relation can then be represented as

$$J^{(2)} = J^{(1)} + \mathrm{d}J^{(1)}. \tag{11}$$

In order to make the updated value of each iteration approach the solution, the updated value $J^{(2)}$ must be less than the initial value $J^{(1)}$, that is $\mathrm{d}J^{(1)} < 0$. Since the performance index J is a function of the $2p$ independent variables ($c_{di}^{(1)}$ and $k_{di}^{(1)}$, $i = 1, 2, \ldots, p$), its total derivative can be taken as

$$\mathrm{d}J^{(1)} = \sum_{i=1}^{p} \left[\frac{\partial J^{(1)}}{\partial c_{di}} \mathrm{d}c_{di}^{(1)} + \frac{\partial J^{(1)}}{\partial k_{di}} \mathrm{d}k_{di}^{(1)} \right]. \tag{12a}$$

Let $\frac{\partial J^{(1)}}{\partial c_{di}} = -\mathrm{d}c_{di}^{(1)}$ and $\frac{\partial J^{(1)}}{\partial k_{di}} = -\mathrm{d}k_{di}^{(1)}$; then Eq. (12a) can be represented as

$$\mathrm{d}J^{(1)} = \sum_{i=1}^{p} [-(\mathrm{d}c_{di}^{(1)})^2 - (\mathrm{d}k_{di}^{(1)})^2] = -\sum_{i=1}^{p} [(\mathrm{d}c_{di}^{(1)})^2 + (\mathrm{d}k_{di}^{(1)})^2] \tag{12b}$$

where $\mathrm{d}J^{(1)}$ is a negative. If $\mathrm{d}c_{di}^{(1)}$ ($c_{di}^{(2)} - c_{di}^{(1)}$) and $\mathrm{d}k_{di}^{(1)}$ ($k_{di}^{(2)} - k_{di}^{(1)}$) are very small, the increments of the parameters $\mathrm{d}c_{di}^{(1)}$ and $\mathrm{d}k_{di}^{(1)}$ are assumed to be, respectively, as follows:

$$\mathrm{d}c_{di}^{(1)} = c_{di}^{(2)} - c_{di}^{(1)} = -s_{ci} \frac{\partial J^{(1)}}{\partial c_{di}}, \quad i = 1, 2, \ldots, p \tag{13a}$$

$$\mathrm{d}k_{di}^{(1)} = k_{di}^{(2)} - k_{di}^{(1)} = -s_{ki} \frac{\partial J^{(1)}}{\partial k_{di}}, \quad i = 1, 2, \ldots, p \tag{13b}$$

where s_{ci} and s_{ki} are, respectively, the steps of the increments for the parameters c_{di} and k_{di}, and the partial differentials ($\frac{\partial J^{(1)}}{\partial c_{di}}$ and $\frac{\partial J^{(1)}}{\partial k_{di}}$) in Eqs. (13a) and (13b) can be obtained from Eqs. (9a) and (9b). Substituting Eqs. (13a) and (13b) into Eq. (12a), the total derivative of the performance index can be written as

$$\mathrm{d}J^{(1)} = -\sum_{i=1}^{p} \left[s_{ci} \left(\frac{\partial J^{(1)}}{\partial c_{di}} \right)^2 + s_{ki} \left(\frac{\partial J^{(1)}}{\partial k_{di}} \right)^2 \right] < 0. \tag{14}$$

From Eq. (14), one ensures that the updated value $J^{(2)}$ of the performance index is always less than its initial value $J^{(1)}$ and the iterated results proceed toward convergent values. The updated values of the TMD design parameters (c_{di} and k_{di}) can be further represented as

$$c_{di}^{(2)} = c_{di}^{(1)} + \mathrm{d}c_{di}^{(1)} = c_{di}^{(1)} - s_{ci} \frac{\partial J^{(1)}}{\partial c_{di}}, \quad i = 1, 2, \ldots, p \tag{15a}$$

$$k_{di}^{(2)} = k_{di}^{(1)} + \mathrm{d}k_{di}^{(1)} = k_{di}^{(1)} - s_{ki} \frac{\partial J^{(1)}}{\partial k_{di}}, \quad i = 1, 2, \ldots, p. \tag{15b}$$

Substituting the updated design parameters $c_{di}^{(2)}$ and $k_{di}^{(2)}$ into Eq. (7), the updated value of the performance index, $J^{(2)}$, can be calculated. Again, let $c_{di}^{(1)} = c_{di}^{(2)}$, $k_{di}^{(1)} = k_{di}^{(2)}$ and $J^{(2)} = J^{(1)} + \mathrm{d}J^{(1)}$, and the above-mentioned procedures are repeated until the convergence of the design parameters is achieved. In other words, the optimal design parameters of the TMD can be obtained from this step-by-step iterative method in which the performance index J in the current iteration is always smaller than the one in the previous iteration. That is, the larger the number of iterations, the closer the results approach the exact solutions. However, in order to take both the accuracy and the computation efficiency into account, iteration processes will be terminated as the error between two consecutive iterated performance indices becomes less than the prescribed tolerance. The flowchart of the proposed numerical method

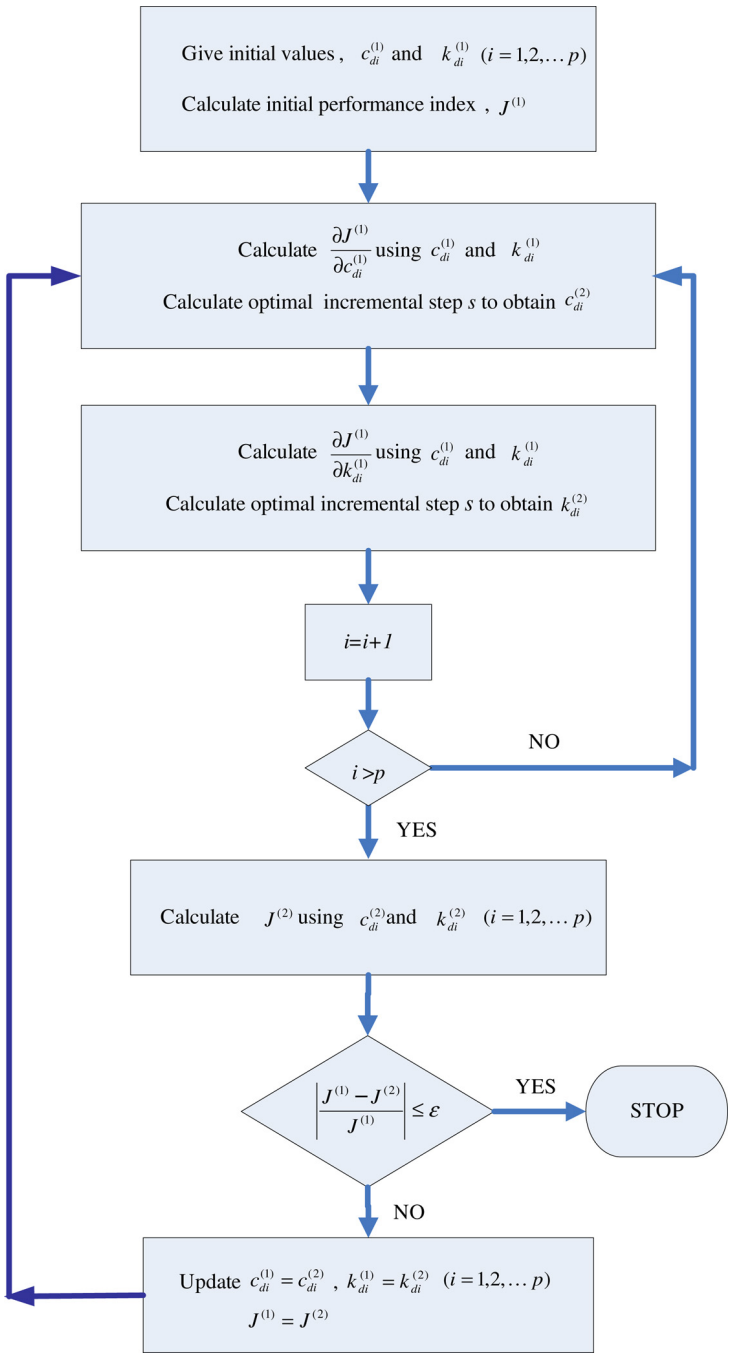

Fig. 1. Flowchart of proposed numerical method.

is shown in Fig. 1. Eqs. (12a) and (12b) is valid only if the incremental step for each design parameter for the TMD is small. However, if the incremental step is too small, the computation efficiency will decrease. On the other hand, if the incremental step is too large, the decrease of the performance index J with the number of iterations will not be ensured. Therefore, the upper bound and the lower bound of the incremental step for each design parameter of the TMD must be determined first, and the golden section search method [24] is then adopted to compute the optimal incremental steps [25] for the proposed numerical method in this paper. The determination of the upper bound and the lower bound of the incremental step is described as follows:

(1) Set the initial upper bound ($s_u = 10^{-9}$) and the initial lower bound ($s_l = 0$) of the incremental step (s).
(2) Substitute s_u and s_l into Eqs. (15a) and (15b) to obtain $c_d^{(S_u)}$, $k_d^{(S_u)}$, $c_d^{(S_l)}$, and $k_d^{(S_l)}$ which in turn are used to calculate $J(s_u)$ and $J(s_l)$, respectively.

(3) If $J(s_u) > J(s_l)$, let $s_u = \frac{s_u}{10}$ and $s_l = s_l$, then go back to step 2.
(4) If $J(s_u) < J(s_l)$, let $s'_l = s_u$ and $s'_u = 10 \times s_u$, and calculate $J(s'_u)$ and $J(s'_l)$, respectively.
(5) Update the upper bound and the lower bound of the incremental step, $s_l = s'_l$, $s_u = s'_u$, and the performance indices, $J(s_u) = J(s'_u)$, $J(s_l) = J(s'_l)$.
(6) If $J(s_u) < J(s_l)$, go back to step 4, otherwise, $s_l = s'_l$, $s_u = s'_u$.

Once the upper bound and the lower bound of the incremental step are obtained, the golden section search method can be used to find the optimal incremental step (s) as follows:

(1) Assign the upper bound (s_u) and the lower bound (s_l) of the incremental step (s)
(2) Let $d = s_u - s_l$, $\rho = (3 - \sqrt{5})/2$ (golden ratio), and the interval $[s_l, s_u]$ can be divided into three segments by $s_1 = s_l + \rho d$ and $s_2 = s_u - \rho d$ which are in turn used to calculate $J(s_1)$ and $J(s_2)$.
(3) Calculate the relative error, $\left|\frac{J(s_2)-J(s_1)}{J(s_1)}\right| \leq \delta$, in which δ is the prescribed tolerance. If the relative error satisfies the aforementioned condition, $s = s_1$; otherwise, $s = s_2$.
(4) If step 3 is not satisfied, update the interval as $d = (1 - \rho)d$.
(5) If $J(s_1) < J(s_2)$, let $s'_2 = s_1$, $J(s'_2) = J(s_1)$, and then calculate $s'_1 = s'_2 - (1 - 2\rho)d$ and $J(s'_1)$.
(6) If $J(s_1) > J(s_2)$, let $s'_1 = s_2$, $J(s'_1) = J(s_2)$, and then calculate $s'_2 = s'_1 + (1 - 2\rho)d$ and $J(s'_2)$.
(7) Update the values, $s_1 = s'_1$, $s_2 = s'_2$, $J(s_1) = J(s'_1)$, $J(s_2) = J(s'_2)$, and go back to step 4.

4. Numerical verifications

The feasibility of using the numerical method for the SDOF structure with a STMD and the MDOF structure with a STMD or MTMDs is numerically verified in this section.

4.1. SDOF structure with a STMD

The accuracy of the proposed numerical method is first examined for an undamped SDOF structure, since exact solutions for the simple system exist. The exact solutions for the optimal design parameters of a STMD for a SDOF system under white noise wind disturbance with zero mean can be obtained as follows [8,9]:

$$f_{\text{opt}} = \sqrt{\frac{1 + \mu/2}{1 + \mu}} \tag{16a}$$

$$\xi_{\text{opt}} = \sqrt{\frac{\mu(1 + 3\mu/4)}{4(1 + \mu)(1 + \mu/2)}} \tag{16b}$$

where f_{opt} is the optimal frequency ratio defined as the ratio of the TMD's frequency to the main structure's natural frequency, ξ_{opt} is the optimal damping ratio of the TMD and

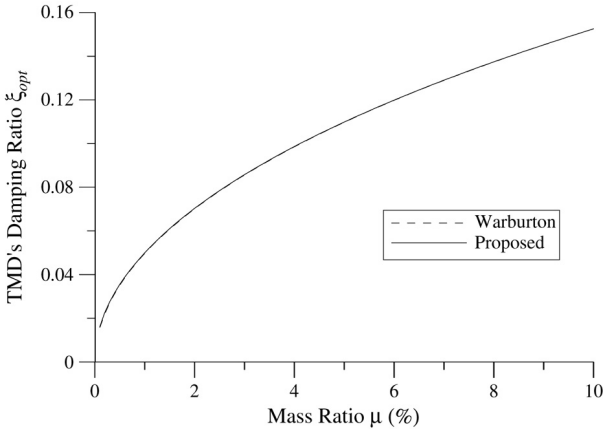

Fig. 2. Variation of optimal damping ratio with mass ratio of the TMD.

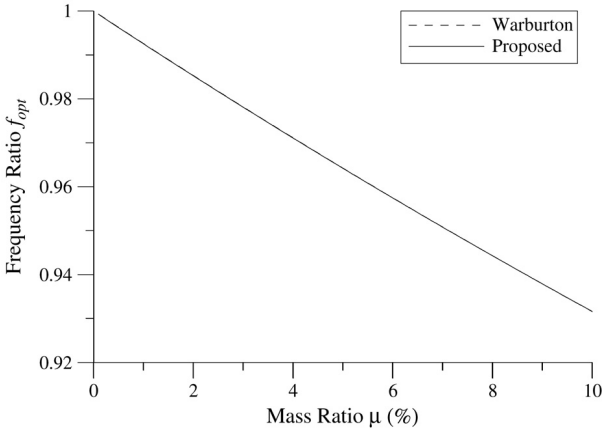

Fig. 3. Variation of optimal frequency ratio with mass ratio of the TMD.

μ is the mass ratio defined as the ratio of the TMD's mass to the main structure's mass. The numerical solutions for these parameters can be obtained by the numerical methods proposed in this paper. As the mass ratio μ of the TMD to the structure increases, the optimal damping ratio ξ_{opt} of the TMD increases (Fig. 2), while the optimal frequency ratio f_{opt} decreases (Fig. 3). The numerical results for the optimal damping ratio and frequency ratio are very consistent with the exact solutions as represented, respectively, in Figs. 2 and 3. Furthermore, the performance index J not only decreases monotonically but also converges very fast when the number of iterations is larger than 5 as shown in Fig. 4 where a SDOF system with $m_s = 100$ kg, $c_s = 314.16$ N s/m ($\xi_s = 5\%$), $k_s = 98\,696.5$ N/m ($f_s = 5$ Hz), and a TMD system with $m_s = 10$ kg, initial guess values $c_d^{(1)} = 0.1c_s$ and $k_d^{(1)} = 0.1k_s$, are used in this numerical simulation.

4.2. MDOF structure with a STMD

The MDOF structure implemented with a STMD is used as a further illustration of the feasibility of using the proposed numerical method. The objective structure considered in this study is a scaled-down five-story steel

Table 1
System parameters of the five-story structure

Mode	1	2	3	4	5
Frequency (Hz)	2.79	9.58	17.83	27.21	36.09
Damping ratio (%)	0.34	3.44	2.63	2.91	3.21
			Mode shapes		
5f	0.5667	−0.4994	0.4455	−0.0868	−0.4943
4f	0.6314	−0.1747	−0.1903	0.0275	0.7257
3f	0.3580	0.2274	−0.7430	−0.2589	−0.4423
2f	0.3247	0.7856	0.4600	−0.2422	0.0356
1f	0.2159	0.2266	−0.0408	0.9306	−0.1794
			System matrices		
Mass matrix (kg)	804.71	0	0	0	0
	0	827.18	0	0	0
	0	0	827.18	0	0
	0	0	0	827.18	0
	0	0	0	0	830.71
Stiffness matrix (N/m)	12 823 632	−15 513 534	5989 005	736 731	1318 464
	−15 513 534	23 139 828	−12 499 902	−329 616	−4979 556
	5989 005	−12 499 902	15 943 212	−2163 105	−1927 665
	736 731	−329 616	−2163 105	5565 213	−5369 013
	1318 464	−4979 556	−1927 665	−5369 013	22 626 765
Damping matrix (N s/m)	4626.89	−4325.23	818.45	−359.93	−53.37
	−4325.23	6713.18	−3369.74	−622.35	−1457.96
	818.45	−3369.74	5817.92	−724.08	−684.05
	−359.93	−622.35	−724.08	3671.98	−1403.12
	−53.37	−1457.96	−684.05	−1403.12	7750.00

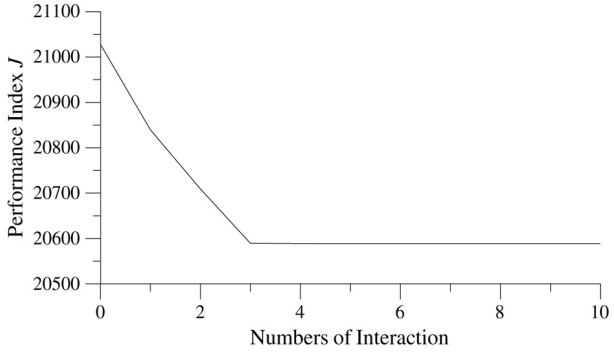

Fig. 4. Convergency of performance index.

frame model. The system parameters of the model structure are summarized in Table 1 [26].

Assuming that a STMD is placed on the roof of the structure for suppressing the vibration induced by earthquakes, and the stroke $x_d(t)$ of the TMD is defined as the displacement relative to the roof, the location vector of the mass for the TMD can be expressed as

$$\mathbf{a} = \begin{bmatrix} 1 & 0 & 0 & 0 & 0 & 1 \end{bmatrix}^{\mathrm{T}}$$

while the location vector of the stiffness and damping for the TMD can be written as

$$\mathbf{b} = \begin{bmatrix} 0 & 0 & 0 & 0 & 0 & 1 \end{bmatrix}^{\mathrm{T}}.$$

In the processes of optimization, only the suppression of structural responses is involved. Therefore, the location matrix of the partial responses of the structure can be represented as

$$\mathbf{D} = \begin{bmatrix} \mathbf{I} & \mathbf{0} \end{bmatrix}_{5\times 6}.$$

Moreover, the weight of the TMD is 123.51 kgf, which is 3% of the structure's total weight.

As the structure is subjected to the earthquake load, the location vector of the external disturbances becomes

$$\mathbf{E} = \begin{bmatrix} \mathbf{M}_s & \mathbf{0} \\ \mathbf{0} & 0 \end{bmatrix} \mathbf{1} + m_d \mathbf{a}$$

where $\mathbf{1} = \begin{bmatrix} 1 & 1 & 1 & 1 & 1 & 1 \end{bmatrix}^{\mathrm{T}}$. Assuming that the earthquake excitation $w(t)$ is a stationary excitation that can be modeled as a white noise signal with constant spectral density, S_0, filtered through the Kanai–Tajimi model [27,28], the PSD function is given by

$$S_{\mathrm{ww}}(f) = \frac{1 + 4\xi_g^2 (f/f_g)^2}{[1 - (f/f_g)^2]^2 + (2\xi_g f/f_g)^2} S_0 \tag{17}$$

where ξ_g and f_g are the ground damping and frequency, respectively. In this paper, $\xi_g = 0.6$ and $f_g = 2.39$ Hz (15 rad/s) are used for numerical simulations. The PSD function and the time history [29] of the Kanai–Tajimi earthquake excitation are shown in Figs. 5a and 5b, respectively. Through the optimization processes,

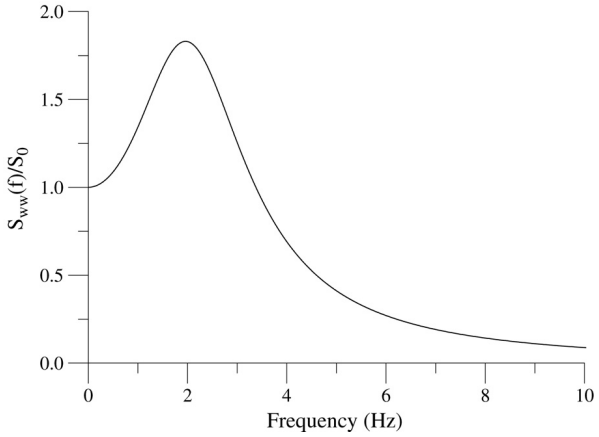

Fig. 5a. Kanai–Tajimi earthquake excitation spectrum.

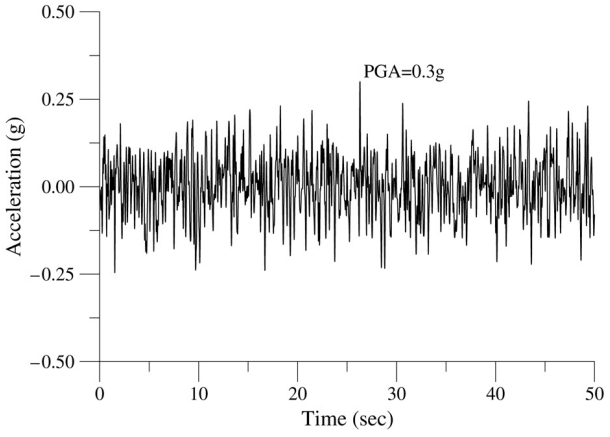

Fig. 5b. Kanai–Tajimi earthquake excitation time history.

the optimal natural frequency ratio f_{opt} is 0.938, the optimal damping ratio ξ_{opt} is 10.84% and the minimal performance index $J_{\min}$ reduces to 6.61% of the original performance index J_{org} which is the mean square value of the structural responses before the implementation of the TMD. The frequency ratio is defined as the ratio of the TMD's natural frequency and the fundamental frequency of the structure.

The equivalent natural frequencies and damping ratios of the 6-DOF system are obtained from the eigenvalue analysis as

$$f = \begin{bmatrix} 2.45 & 2.98 & 9.59 & 17.84 & 27.22 & 36.10 \end{bmatrix} \quad \text{(Hz)}$$
$$\xi = \begin{bmatrix} 6.14 & 5.19 & 3.56 & 2.68 & 2.91 & 3.24 \end{bmatrix} \quad (\%).$$

It is observed that the natural frequencies of the structure are only slightly changed as the TMD is implemented, while the equivalent damping ratios are enhanced, especially for the first two coupled modes.

The effectiveness of the TMD is also revealed from the frequency response function of the roof displacement (Fig. 6) where the peak frequency response at 2.79 Hz without the TMD is greatly suppressed as the TMD is installed. The result is consistent with that from the eigenvalue analysis.

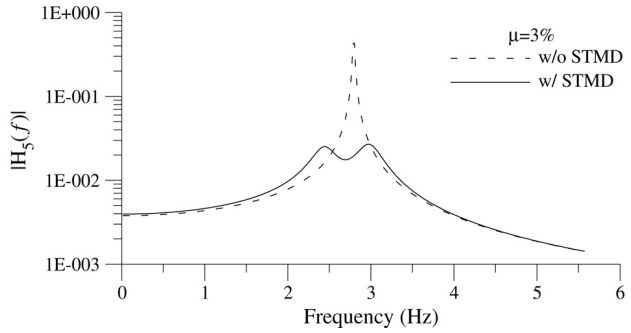

Fig. 6. Roof displacement frequency response function (STMD, Kanai–Tajimi earthquake force).

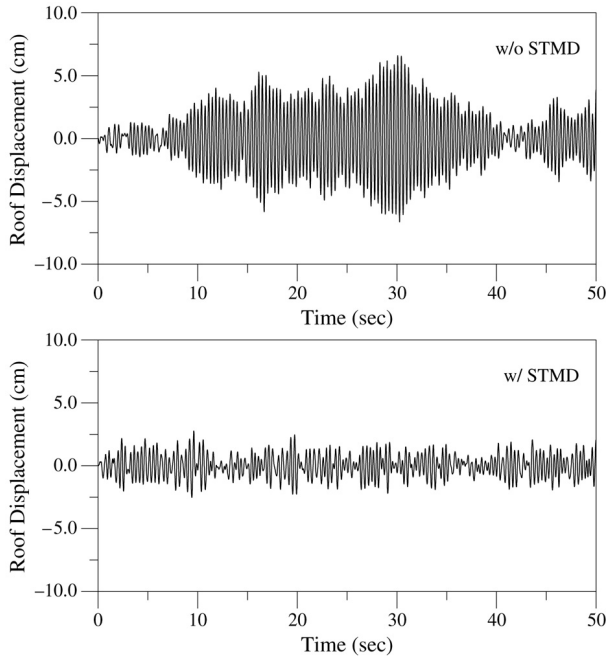

Fig. 7. Comparison of roof displacement response (STMD, Kanai–Tajimi earthquake force).

The roof displacement of the structure with and without the TMD is illustrated in Fig. 7. Good reduction in structural response has been achieved if the parameters of the TMD are adopted through the optimal design procedures.

For further numerical verification of the proposed method, a ten-story shear building implemented with a STMD (on the roof) under the El Centro earthquake is also analyzed in this paper, and the results are compared with those studied by Hadi et al. [21] using the genetic algorithm (GA) to minimize the H_2 norm of the transfer function of the system. The fundamental frequency and damping ratio of the building are 1.011 Hz and 3.03%, respectively. In addition, the mass of the STMD is specified to be 3% of the structure's total mass and the initial guess values $c_d^{(1)} = 0.001c_1$ and $k_d^{(1)} = 0.0001k_1$ for the STMD are adopted in this simulation. Through the optimization processes, the optimal natural frequency ratio f_{opt} is 0.973 ($k_d = 4126.93$ kN/m) and the optimal damping ratio ξ_{opt} is

Table 2
Peak response of the roof for ten-story building under El Centro earthquake

Floor	Genetic algorithm (Hadi)		Proposed method	
	Displacement (m)	Acceleration (m/s^2)	Displacement (m)	Acceleration (m/s^2)
1	0.019	2.698	0.020	2.672
2	0.037	3.025	0.039	3.097
3	0.058	3.528	0.057	3.638
4	0.068	3.944	0.073	3.989
5	0.082	4.079	0.087	4.122
6	0.094	3.826	0.099	4.139
7	0.104	4.390	0.108	4.262
8	0.113	5.051	0.117	4.951
9	0.119	5.534	0.123	5.438
10	0.122	5.812	0.126	5.720
TMD	0.358	13.942	0.282	11.659

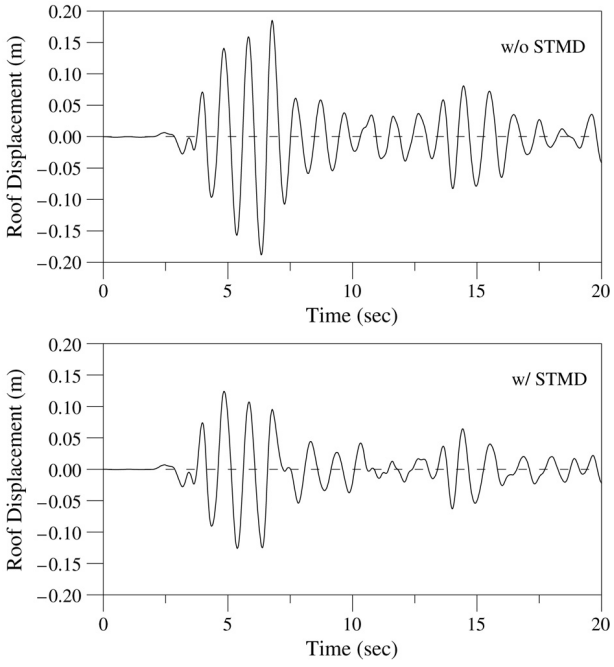

Fig. 8. Comparison of roof displacement response (STMD, El Centro earthquake force).

20.36% ($c_d = 271.79$ kN s/m), while $f_{\text{opt}} = 0.928$ ($k_d = 3750$ kN/m) and $\xi_{\text{opt}} = 11.9\%$ ($c_d = 151.5$ kN s/m) are obtained by the GA method under the predefined restraint conditions, $k_d = 0$–4000 kN/m and $c_d = 0$–1000 kN s/m. The peak responses of the roof for the ten-story building installed with a STMD on the roof are summarized in Table 2 where the peak structural responses obtained by the proposed method are close to those obtained from the GA method, except as regards the peak responses of the TMD which are smaller than Hadi's results due to the large damping ratio obtained by the proposed method. The roof displacement of the ten-story structure with and without a STMD is illustrated in Fig. 8 where the peak displacement reduction of 33% has been achieved.

4.3. MDOF structure with MTMDs

The feasibility of the proposed numerical method for the MDOF structure implemented with two TMDs on the roof and the third floor to suppress the vibration against wind load is further illustrated. If the structure is subjected to the wind load, the external disturbance profile against the floor height of the structure is determined by the power law [30] as

$$\mathbf{e} = \begin{bmatrix} 1.00 & 0.94 & 0.86 & 0.77 & 0.64 \end{bmatrix}^{\mathrm{T}}$$

where the element of the profile for the roof is normalized to 1.0. Moreover, the system parameters shown in Eq. (2) can be expressed as

$$\mathbf{M} = \begin{bmatrix} \mathbf{M}_s & \mathbf{0} \\ \mathbf{0} & \mathbf{0} \end{bmatrix} + \sum_{i=1}^{2} m_{di}\mathbf{a}_i\mathbf{a}_i^{\mathrm{T}} \text{ is the } 7 \times 7 \text{ mass matrix,}$$

$$\mathbf{C} = \begin{bmatrix} \mathbf{C}_s & \mathbf{0} \\ \mathbf{0} & \mathbf{0} \end{bmatrix} + \sum_{i=1}^{2} c_{di}\mathbf{b}_i\mathbf{b}_i^{\mathrm{T}} \text{ is the } 7 \times 7 \text{ damping matrix,}$$

$$\mathbf{K} = \begin{bmatrix} \mathbf{K}_s & \mathbf{0} \\ \mathbf{0} & \mathbf{0} \end{bmatrix} + \sum_{i=1}^{2} k_{di}\mathbf{b}_i\mathbf{b}_i^{\mathrm{T}} \text{ is the } 7 \times 7 \text{ stiffness matrix,}$$

in which

$$\mathbf{a}_5 = \begin{bmatrix} 1 & 0 & 0 & 0 & 0 & 1 & 0 \end{bmatrix}^{\mathrm{T}}, \quad \mathbf{a}_3 = \begin{bmatrix} 0 & 0 & 1 & 0 & 0 & 0 & 1 \end{bmatrix}^{\mathrm{T}},$$
$$\mathbf{b}_5 = \begin{bmatrix} 0 & 0 & 0 & 0 & 0 & 1 & 0 \end{bmatrix}^{\mathrm{T}}, \quad \mathbf{b}_3 = \begin{bmatrix} 0 & 0 & 0 & 0 & 0 & 0 & 1 \end{bmatrix}^{\mathrm{T}},$$

$\mathbf{E} = \begin{bmatrix} \mathbf{I}_{5\times5} \\ \mathbf{0}_{2\times5} \end{bmatrix}$ is the 7×5 location matrix of external wind loads and the PSD function of external wind loads can be represented as $S_{\text{WW}}(\omega) = S_0 S_u(\omega)$ where $S_u(\omega)$ is the Davenport along-wind speed spectrum as shown in Fig. 9(a) and its time history is shown in Fig. 9(b). Through the optimization processes, the optimal natural frequency ratio f_{opt} and the optimal damping ratio ξ_{opt} for the TMD on the roof are 1.027% and 7.94%, respectively, and those on the third floor are 0.958% and 4.07%, respectively.

The equivalent natural frequencies and damping ratios of the 7-DOF passive controlled system are obtained from the

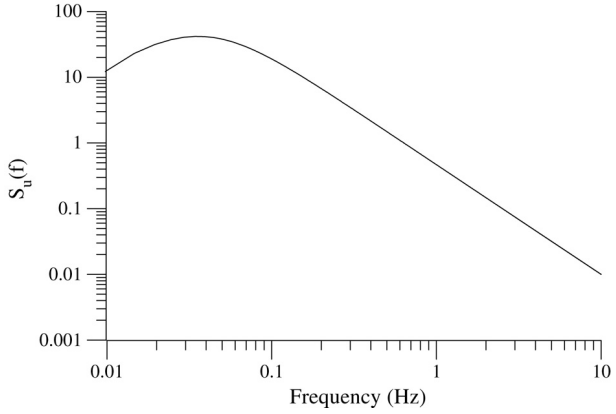

Fig. 9(a). Davenport along-wind speed spectrum.

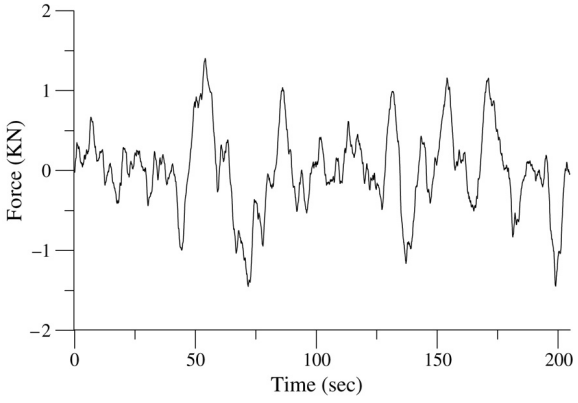

Fig. 9(b). Davenport along-wind force time history.

eigenvalue analysis as

$$f = \begin{bmatrix} 2.59 & 2.75 & 3.00 & 9.58 & 17.84 & 27.22 & 36.09 \end{bmatrix} \quad \text{(Hz)}$$
$$\xi = \begin{bmatrix} 3.02 & 4.75 & 5.12 & 3.48 & 2.66 & 2.91 & 3.22 \end{bmatrix} \quad (\%).$$

It is observed that the natural frequencies of the structure are only slightly changed, while the equivalent damping ratios are enhanced, especially for the first three coupled modes.

The effectiveness of the TMD is also revealed from the displacement frequency response functions of the roof and the third floor, respectively, in Figs. 10 and 11 where the peak frequency response at 2.79 Hz without TMD control is greatly suppressed as two TMDs are installed. The result is also consistent with that from the eigenvalue analysis.

The roof acceleration of the structure with and without two TMDs is illustrated in Fig. 12 where good reductions of the structural responses has been achieved as the structure is implemented with two TMDs.

5. Concluding remarks

In this paper, an optimal design theory for the TMD is developed, and the feasibility of the proposed method has been verified via numerical simulations. During the process of deriving the optimal design, the proposed method takes into account various conditions, such as full states of the dynamic system of MDOF structures, MTMDs, and the frequency distribution and allocation of environmental disturbances. Consequently, the proposed method allows for

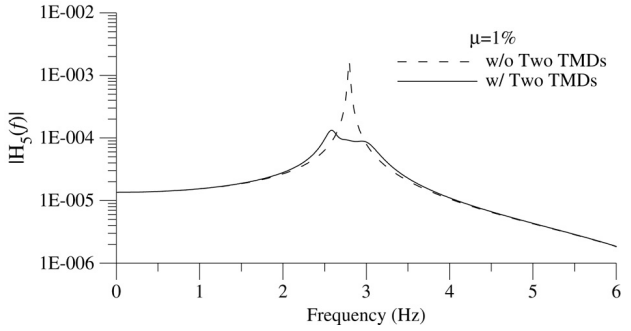

Fig. 10. Roof displacement frequency response function (two TMDs, Davenport along-wind force).

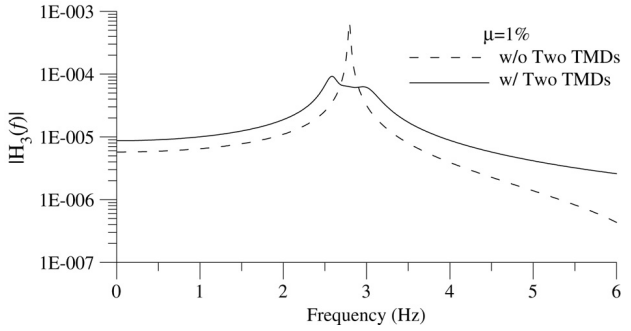

Fig. 11. Third-floor displacement frequency response function (two TMDs, Davenport along-wind force).

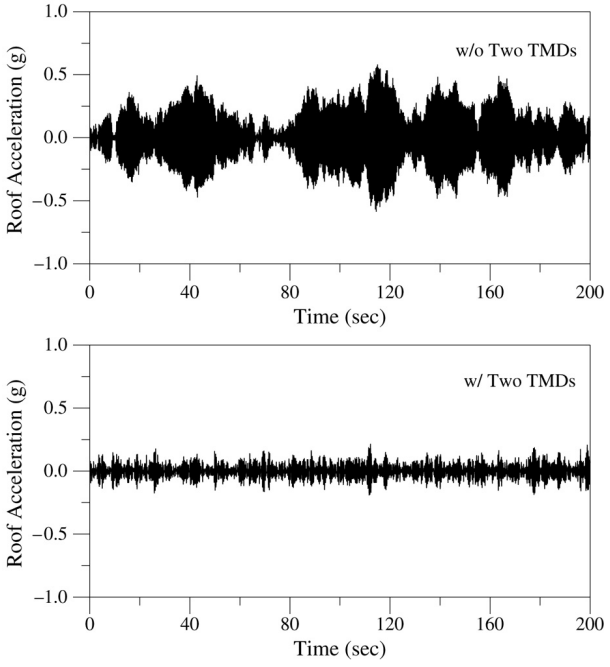

Fig. 12. Comparison of roof acceleration response (two TMDs, Davenport along-wind force).

more extensive applications of the TMD. The optimal design parameters of the TMD are systematically determined to minimize the mean square value of the structural responses in the frequency domain. Since the sufficient and necessary conditions for the optimization of the TMD parameters are a set of highly nonlinear simultaneous equations, the exact solution of the optimal design parameters is difficult to obtain, except for the undamped SDOF structure with a STMD. Therefore, this study introduces a numerical method to search for the optimal design parameters of the TMD in a systematic fashion. With the proposed numerical method, the numerical solution converges monotonically and very effectively toward the exact solutions as the number of iterations increases. Moreover, the proposed optimal design theory is derived by using full states of the dynamic system without any model order reduction. Therefore, the error introduced by the mathematical model can be reduced, and the control effectiveness of the TMD can also certainly be guaranteed.

References

[1] McNamara RJ. Tuned mass dampers for buildings. Journal of the Structure Division, ASCE 1977;103:1985–98.

[2] Luft RW. Optimal tuned mass dampers for buildings. Journal of the Structure Division, ASCE 1979;105:2766–72.

[3] Haskett T, Breukelman B, Robinson J, Kottelenberg J. Tuned mass dampers under excessive structural excitation. Report of the Motioneering Inc. Guelph, Ontario, Canada N1K 1B8.

[4] Frahm H. Device for damping vibration of bodies. U.S. Patent No. 989-958; 1911.

[5] Den Hartog JP. Mechanical vibrations. 4th ed. NY: McGraw Hill; 1956.

[6] Fujino Y, Abe M. Design formulas for tuned mass dampers based on a perturbation technique. Earthquake Engineering and Structural Dynamics 1993;22:833–54.

[7] Crandall SH, Mark WD. Random vibration in mechanical systems. NY: Academic Press; 1973.

[8] Warburton GB. Optimum absorbers for simple systems. Earthquake Engineering and Structural Dynamics 1980;8:197–217.

[9] Warburton GB. Optimum absorber parameters for various combinations of response and excitation parameters. Earthquake Engineering and Structural Dynamics 1982;10:381–401.

[10] Rana R, Soong TT. Parametric study and simplified design of tuned mass dampers. Engineering Structures 1998;20:193–204.

[11] Fujino Y, Abe M. Dynamic characterization of multiple tuned mass dampers and some design formulas. Earthquake Engineering and Structural Dynamics 1994;23:813–35.

[12] Jangid RS, Datta TK. Performance of multiple tuned mass dampers for torsionally coupled system. Earthquake Engineering and Structural Dynamics 1997;26:307–17.

[13] Xu K, Igusa T. Dynamic characteristics of multiple substructures with closely spaced frequencies. Earthquake Engineering and Structural Dynamics 1992;21:1059–70.

[14] Gu M, Chen SR, Chang CC. Parametric study on multiple tuned mass dampers for buffeting control of Yangpu bridge. Journal of Wind and Areodynamics 2001;89(11–12):987–1000.

[15] Park J, Reed D. Analysis of uniformly and linearly distributed mass dampers under harmonic and earthquake excitation. Engineering Structures 2001;23(7):802–14.

[16] Li C. Performance of multiple tuned mass dampers for attenuating undesirable oscillations of structures under the ground acceleration. Earthquake Engineering and Structural Dynamics 2000;29(9): 1405–21.

[17] Li C, Liu Y. Ground motion dominant frequency effect on design of multiple tuned mass dampers. Journal of Earthquake Engineering 2004;8:89–105.

[18] Li C. Optimal multiple tuned mass dampers under the ground acceleration based on DDMF and ADMF. Earthquake Engineering and Structural Dynamics 2002;31(4):897–919.

[19] Li C, Liu Y. Optimal multiple tuned mass dampers under the ground acceleration based on the uniform distribution of system parameters. Earthquake Engineering and Structural Dynamics 2003;32: 671–90.

[20] Kitts L, Wang BP, Pilkey WD. Vibration reduction over a frequency range. Journal of Sound and Vibration 1983;89(4):559–69.

[21] Hadi MNS, Arfiadi Y. Optimal design of absorber for MDOF structures. Journal of Structural Engineering 1998;124(11):1272–80.

[22] Stech DJ. H_2 approach for optimally tuning passive vibration absorbers to flexible structures. Journal of Guidance, Control, and Dynamics 1994;17:636–8.

[23] Zou L, Nayfeh SA. Minimax optimization of multi-degree-of-freedom tuned-mass dampers. Journal of Sound and Vibration 2004;272: 893–908.

[24] Mathews JH. Numerical methods for mathematics, science, and engineering. 2nd ed. NJ: Prentice Hall; 1992.

[25] Chung LL, Wu LY, Huang KY, Lee MC, Shaw KY. Experimental verification of full-scale active structural control. Structural Engineering, Chinese Society of Structural Engineering 2002;16:67–84 [in Chinese].

[26] Lee CL, Wang YP. Seismic structural control using an electric servomotor active mass driver system. Earthquake Engineering and Structural Dynamics 2004;33:737–54.

[27] Kanai K. An empirical formula for the spectrum of strong earthquake motions. Bulletin Earthquake Research Institute, University of Tokyo 1961;39:85–95.

[28] Tajimi H. A statistical method of determining the maximum response of a building structure during an earthquake. In: Proceeding of II world conference in earthquake engineering; 1960, p. 781–97.

[29] Shinozuka M, Jan CM. Digital simulation of random process and its application. Journal of Sound and Vibration 1972;25:111–28.

[30] SimiuLi E, Scanlan RH. Wind effects on structures, fundamental and applications to design. 3rd ed. NY: John Wiley and Sons Inc.; 1996.